THE UNIVERSITY of EDINBURGH

Edinburgh Research Explorer

Force and pressure investigation of modern asymmetric spinnakers

Citation for published version:
Viola, IM & Flay, RGJ 2009, 'Force and pressure investigation of modern asymmetric spinnakers', *Transactions of the Royal Institution of Naval Architects Part B: International Journal of Small Craft Technology*, vol. 151, no. 2, pp. 31-40. https://doi.org/10.3940/rina.ijsct.2009.b2.98

Digital Object Identifier (DOI):
10.3940/rina.ijsct.2009.b2.98

Link:
Link to publication record in Edinburgh Research Explorer

Document Version:
Early version, also known as pre-print

Published In:
Transactions of the Royal Institution of Naval Architects Part B: International Journal of Small Craft Technology

General rights
Copyright for the publications made accessible via the Edinburgh Research Explorer is retained by the author(s) and / or other copyright owners and it is a condition of accessing these publications that users recognise and abide by the legal requirements associated with these rights.

Take down policy
The University of Edinburgh has made every reasonable effort to ensure that Edinburgh Research Explorer content complies with UK legislation. If you believe that the public display of this file breaches copyright please contact openaccess@ed.ac.uk providing details, and we will remove access to the work immediately and investigate your claim.

Download date: 05. May. 2023

FORCE AND PRESSURE INVESTIGATION OF MODERN ASYMMETRIC SPINNAKERS

I M Viola, **R G J Flay**, Yacht Research Unit, Mechanical Engineering Department, The University of Auckland, New Zealand

SUMMARY

An innovative pressure system was used at the Yacht Research Unit's Twisted Flow Wind Tunnel (University of Auckland) to test three asymmetrical spinnakers. The sails were designed for the most recent America's Cup Rule (AC33) and tested on a large-scale model. Force measurements were used to determine the sail characteristics, optimum apparent wind angles and resulting heel angles. Pressures were firstly measured on 5 chord-wise sections with 11 pressure taps on each section, which enabled mapping of the pressure on the sail surface. Measurements were performed between apparent wind angles of 40° and 70° and heel angles between 0° and 20°. The pressure measurements are discussed and related to the flow field around the sails. In particular the pressure on the leeward side of the asymmetric spinnaker is correlated to the leading edge separation and reattachment, and to the trailing edge separation. Subsequently 34 pressure taps were used to measure the pressure on a single section of the asymmetric spinnaker. This allowed an investigation of the effect of the sail trim on the resulting pressure distribution. The results verified that the three sails were suited for their intended design purpose. Over-trimming to reduce luff flapping was also investigated. It was found to reduce both drag and rolling moment. Further successive over-trimming showed a reduction in the leeward suction on the spinnaker, with the pressure distribution becoming more uniform as the flow became more separated.

NOMENCLATURE

AC	America's Cup
AC33	33rd America's Cup Class (second hypothesis)
AC90	33rd America's Cup Class (first hypothesis)
AWA	Apparent wind angle
AWS	Apparent wind speed
CFD	Computational fluid dynamics
CMx	Roll moment coefficient, x-axis lies on the water plane (-)
Cp	Pressure coefficient (-)
Cx	Drive force coefficient (-)
DOG	Deed of Gift
Fx	Drive force, along the longitudinal axis of the model, positive in the boat direction (N)
h	Model height (m)
IACC	International America's Cup Class
Mid-section	Horizontal section of the sails at 1/2 of the mitre height
Mitre	Line made up of the points on the sail surface equally far from the leech and the luff
q	Dynamic pressure coefficient (Pa)
SA	Sail area (m^2)
TWS	True wind speed
VMG	Velocity made good
VO70	Volvo Ocean Race Open 70 Class
W60	Whitbread 60 Class

1. INTRODUCTION

The aerodynamics of asymmetrical spinnakers is a modern science that has became of particular interest with the recent America's Cup races. Until the end of the 1990s a symmetrical spinnaker tacked onto a spinnaker pole was generally more common than asymmetric spinnakers. The Whitbread 60 class (W60) was one of the first yacht classes to largely adopt asymmetric spinnakers for the Whitbread Round the World Race in 1993/1994, which were tacked onto the end of the spinnaker pole. The W60s were also used for the last Whitbread in 1997/1998, and were renamed Volvo Ocean 60s when the race became the Volvo Ocean Race in 2001/2002. The following edition in 2005/2006 was sailed with the new Volvo Open 70 (VO70) that had a bowsprit. The spinnaker pole became optional and only a few teams opted to carry one. For the latest edition of the race in 2008/2009, the VO70 carried only asymmetric spinnakers tacked to the bowsprit.

Symmetrical spinnakers were still largely used in the 31st edition of the America's Cup (AC) sailed with the International America's Cup Class (IACC) in Auckland in 2003. In the following AC sailed with the IACC yachts in Valencia in 2007, symmetrical spinnakers were used significantly less than asymmetrics, both of which were tacked to the pole in the absence of a bowsprit. It appears at the present time that the format of the 33rd AC will be a "Dead Of Gift" (DOG) match in multi-hulls, but before that became clear, two new class rules were developed: the AC90 and the AC33 classes. Both of these rules would lead to much faster boats than the previous IACC design. They are to have long bowsprits and will sail only asymmetric spinnakers.

The history of two of the most important races in the yachting world, the America's Cup and the Volvo Ocean Race, shows that the asymmetric spinnaker will perhaps become a substitute for symmetrical spinnakers in the future of the mainstream yachting.

Symmetrical spinnaker aerodynamics has been investigated in previous research but is still far from being fully understood. On the contrary, there are only a few published papers on the aerodynamics of asymmetric spinnakers.

Most of the research on sails has been performed by measuring the global aerodynamic forces (using force balances) which gives very limited information about the flow field around the sails. In recent years, Computational Fluid Dynamics (CFD) has allowed computation of the complex separated flow fields around downwind sails. Unfortunately, to validate the CFD results a simplified geometry, which is generally not representative enough of the complex aerodynamics of

the sail, has often been used. Alternatively, CFD has been validated with the global forces measured in the wind tunnel, which does not verify that the correct flow field was computed. In the present wind tunnel investigation the overall forces and moments have been measured, as well as the pressure map on the asymmetric spinnakers, allowing a deeper understanding of the flow field around the sails.

2. STATE OF THE ART

The state of the art of force measurements on sails up to the mid 1990s is well described by Marchaj [1] and since then by Claughton & Campbell [2] who describe the research activities of the Yacht Research Group at the University of Southampton and the Wolfson Unit for Marine Technology. In particular, [2] presents the force measurements performed on a W60 from 24° to 65° apparent wind angle (AWA).

In 1992, the Yacht Research Unit (YRU) of the University of Auckland pointed out the need to perform wind tunnel tests of downwind sails with an incoming twisted flow to simulate the real-life incoming flow on a sailing yacht [3]. The design of the YRU's special wind tunnel with twisted flow for testing yacht sails, which was built in 1994, is described in [4]. The different results of testing with or without the twisted flow were computed with CFD [5]. In 2003, a new wind tunnel test procedure was developed by the YRU which links the measured aerodynamic forces to a Velocity Prediction Program (VPP), which computes the boat speed and the heel angle corresponding with the measured forces [6]. Hence, the model is heeled in real-time and the sails can be trimmed to optimise the boat speed. Some years later, the first author of the present paper developed at the Politecnico di Milano Wind Tunnel a similar device to perform downwind sail tests with twisted flow [7] and set up a testing procedure with integrated VPP which allowed heeling of the model in real-time [8].

The first work published on asymmetric spinnakers was performed in 1999 at the Glenn L. Martin Wind Tunnel at the University of Maryland in uniform flow by Ranzenbach et al [9], who questioned the need to test with twisted flow. The authors described the sail inventory of the W60 named *Swedish Match* for a range of wind speeds from 5 to 40 knots and true wind angles (TWA) from 20° to 180°. The sails were divided into groups of symmetric spinnakers, running asymmetrics and reaching asymmetrics, where running asymmetrics had significantly larger sail areas than the reaching asymmetrics. The results of the measurements were presented in [10] which showed the cross-over between these three sail categories, concluding that the reaching asymmetrics should be sailed between 55° and 100° AWA, the running asymmetrics between 100° and 140° AWA, and the symmetric spinnaker between 140° and 180° AWA. In the same wind tunnel, the performances of downwind sails adopted by the International Measurement System (IMS) fleet were investigated deeply. Ranzenbach & Teeters compared symmetric and asymmetric spinnakers tacked onto a spinnaker pole or bowsprit, between 80° and 150° AWA [11]. They also investigated the differences between masthead and fractional spinnakers coupled with large or small mainsails [12].

The YRU also carried out much research on both symmetric and asymmetric spinnaker aerodynamics, mainly on AC and Volvo classes. The asymmetric spinnakers of a VO60 were measured between 80° and 110° AWA at several heel angles up to 40° heel [13]. Semi-rigid sails of the VO60 were used in [14] to investigate the interaction between mainsail and asymmetric spinnaker for apparent wind angles from 80° to 110°. Symmetric spinnakers were tested in preparation for the successful Team New Zealand challenge in the 30th AC [15]. The IACC velocity polars were investigated concluding that the normal downwind AWA's were between 90° and 135° in wind speeds over 5m/s.

Symmetrical spinnakers were also investigated in [16] and [17] and the separated region on the leeward side of the spinnaker was shown with tufts which were illuminated with ultra violet light and photographed [17]. The first pressure measurements on symmetrical spinnakers were recently published [18]. It was performed at the YRU wind tunnel on 7 horizontal sections of a 1/25th scale IACC spinnaker, with 8 pressure taps on each section, sailing at 120° AWA. Measurements were compared with CFD results and general similarities and some differences were observed.

The pressure distributions on the asymmetric spinnakers used by Lunarossa Challenger in the 32nd AC were recently investigated with high grid resolution CFD by the principal author in [19] and [20]. The same sail designs were also tested at the Politecnico di Milano Wind Tunnel in 2006 and 2007 [21] and the forces computed with CFD showed good agreement with the wind tunnel measurements for the three AWA's investigated (45°, 105° and 120°).

3. YRU EXPERIMENTS

3.1 Model Selection

As noted above, in 2007 and 2008 it was expected that the 33th AC would possibly be sailed with the AC33 yacht design, which is lighter and has more righting moment than the IACC, and hence would be faster. The AC33 spinnaker dimensions are limited only by a maximum edge length of 45m, allowing effectively an unlimited downwind sail area. These boats would sail the downwind course at relatively tight AWA's with large asymmetric spinnakers tacked onto the bowsprit. The YRU has performed some preliminary tests for Emirates Team New Zealand on several asymmetric spinnakers on a 1/15th scale AC33 model. As this model and several sails were available, it was decided that it would be used

for the present asymmetric spinnaker force and pressure investigation.

3.2 Sail specifications, and test configurations

The three asymmetric spinnakers tested were labelled A1, A2 and A3, respectively. The A1 had the smallest sail area and was designed for light wind reaching with flat sections; the A2 had an intermediate sail area and was a general purpose sail; the A3 had the largest sail area and was designed for running deep in stronger wind and had deep sections. Table 1 summarize the main dimensions of the sails.

Table 1: 1/15th scale model sail dimensions.

	Mainsail	A1	A2	A3
Luff	0.21m	2.15m	2.44m	2.49m
Mitre	-	2.35m	2.40m	2.48m
Leach	-	2.45m	2.14m	2.15m
Foot	0.62m	1.44m	1.44m	1.50m
Sail Area	0.9m^2	2.4m^2	2.6m^2	3.0m^2

Each sail was tested in 5 configurations: at 40°, 55°, 70° AWA and 10° heel; and at 0°, 10°, 20° heel and 55° AWA. Conventional cloth sails were used so as to be able to trim the sail for the maximum drive force. For each condition, two spinnaker sheeting trims were considered: the trim maximising the drive force which can lead the luff to flap, and a tighter trim required to stabilise the luff and stop it flapping.

3.3 Pressure measurement system, and pressure tap locations

A pressure system capable of acquiring up to 512 pressure taps simultaneously at high frequency was used for the investigation. Pressures were acquired for 70s at 100Hz. Customised plastic pressure taps were made and attached to the sails on 5 horizontal sections at 1/8, 1/4, 1/2, 3/4 and 7/8 of the mitre (line made up of the points on the sail surface equally far from the leech and the luff). Eleven pressure taps were located on each section: at 1/12, 1/6, 1/4, 3/8, 1/2, 5/8, 3/4, 5/6, 11/12 of the curve length, plus one as close as possible to the luff and one as close as possible to the leech. To minimise the number of tubes on the model that could affect the aerodynamics, the pressure distribution was measured on one sail surface at a time, hence 5x11=55 pressure measurements were recorded simultaneously. A successive set of pressure measurements was performed to investigate in more detail the pressure distribution on the mid-section of the sails (horizontal section at 1/2 of the mitre height). 34 unequally spaced pressure taps were used on the same section.

The pressure taps were made by securing the tap onto the opposite side of the sail surface being measured and connecting it to the measurement side via a small hole in the sail to transmit the pressure. This eliminated any disturbance to the flow on the measurement side. Figure 1 shows the pressure taps on the 2 lowest sections of the spinnaker. The taps and the pressure tubes are much smaller then the characteristic dimension of the sail and they are immersed in the boundary layer of the sail surface. Moreover, the boundary layer affected by the presence of the taps and tubes, is on the opposite sail face to the one where the pressure is measured. Each pressure tap was connected with an equal length of tubing to a Honeywell XSCL04DC temperature compensated differential pressure transducer. All the transducers were pneumatically connected to a reference static pressure measured with a Pitot-static probe located approximately 10m upstream and at the topmast height. The total pressure from the Pitot-static probe was connected to an additional transducer, which measured the reference dynamic pressure q.

Figure 1: Pressure measurement on the leeward side of the spinnaker, showing tubes etc. on the windward side.

The tests were performed in uniform flow (without twisting vanes) but all of the configurations measured with the A3 were re-measured with the twisted flow to investigate how the twisted flow changed the pressure distribution on the spinnaker. The reference wind speed was roughly 3.5m/s giving a Reynolds number based on the model height h equal to $6*10^5$. This is less than the full-scale Re by a factor of about 20. In uniform flow, the turbulence intensity was lower than 3% and the boundary layer was confined to the first 10% of the height of the model. In this paper, because of the restricted space available, only the results obtained with uniform flow are presented and discussed.

3.4 Force and moment measurement system

The model was fixed to a 6-component balance via 3 brackets and the hull was partially immersed in a pool of water to act as an airtight seal between the hull and the wind tunnel floor. The forces and moments measured by the balance were transformed into non-dimensional coefficients by dividing the forces by the product of q and SA, and by dividing the moments by the product of q, SA and the height of the model h. Forces and moments were acquired for 70s at 200Hz.

4. RESULTS & DISCUSSION

4.1 Performance at Various AWA's

The differences between the three spinnakers should be evaluated in terms of the maximum speed that the boat can achieve with each sail. This comparison could be performed by running a VPP in-line with the wind tunnel tests [6]. Then at every AWA the sails would be trimmed to maximise the boat speed while the heel angle was automatically changed to balance the measured rolling moment. Having said that, to better understand the physics of each sail, a simpler comparison is performed in the present research which does not involve an excessive number of parameters and knowledge of the hydrodynamics of the yacht. In the following discussion the sails are evaluated in terms of the maximum drive force coefficient *Cx* multiplied by the sail area *SA*, and the corresponding roll moment coefficient *CMx* multiplied by sail area *SA*, i.e. in terms of thrust and rolling moment areas respectively.

Figure 2 shows the maximum *CxSA* achieved at 3 AWA's by each sail configuration. The sails were trimmed to maximise *CxSA* and, in the case of the A3, it was achieved with a flapping luff. The dotted line in the figure shows the force measurements achieved by tightening the A3's sheet just enough to avoid the flapping (Similarly for Figs. 3 – 5.). The A1 gives the maximum thrust at low AWA's while the A3 gives the maximum thrust at high AWA's. The A2 trend suggests that between 40° and 55° there is a region where the A2 is the sail which would provide the maximum thrust. This result is in agreement with the intention of the sail designer who is known to have designed the A1 for light air and close AWA's, the A3 for a stronger breeze and deep AWA's, and the A2 for intermediate conditions.

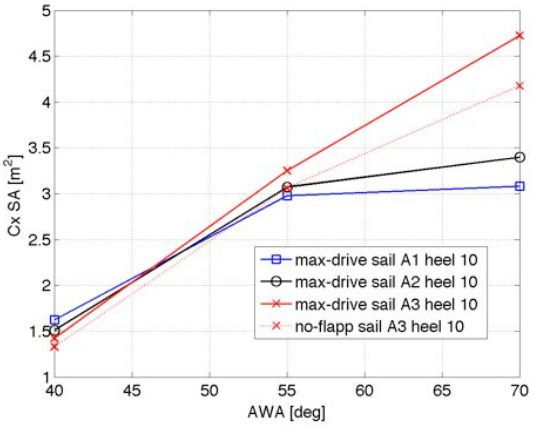

Figure 2: Maximum *CxSA* measured for sails A1, A2 and A3 at 40°, 55° and 70° AWA at 10° heel.

Figure 3 shows the corresponding *CMxSA* for the 3 sails at the 3 AWA's. The A3 gives the largest *CMxSA* and the A1 the smallest. As a consequence, in the same wind conditions the A1 would heel the boat less than the A3. How much the boat would heel at full scale depends on the hydrodynamics of the hull and on the full-scale TWS.

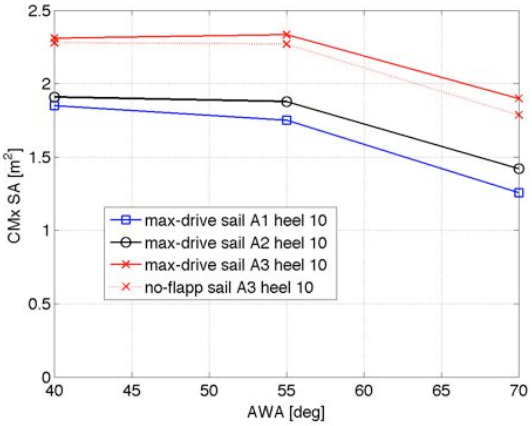

Figure 3: *CMxSA* measured for sails A1, A2 and A3 at 40°, 55° and 70° AWA at 10° heel.

4.2 Performance at Various Heel angles

In sailing upwind, the effect of heel is partially comparable to reductions in the AWA and AWS. The sail trim does not change significantly when the boat heels, hence the geometry of the sail is approximately the same. If we assume that the component of the wind speed in the direction parallel to the mast does not affect the aerodynamics of the sails significantly [22], then the aerodynamic forces should decrease due to the increasing heel. In fact, the apparent wind speed $AWS_{\perp}$ and the apparent wind angle $AWA_{\perp}$ perpendicular to the mast are reduced by the heel angle according to the following equations:

$$AWS_{\perp} = AWS\sqrt{\left(\cos(AWA)\right)^2 + \left(\sin(AWA)\cdot\cos(heel)\right)^2}$$

$$AWA_{\perp} = \arctan\left(\frac{\sin(AWA)\cdot\cos(heel)}{\cos(AWA)}\right)$$

For instance, in a wind speed of 3.5m/s at 55° AWA, heeling the boat by 20° leads to a theoretical reduction of 2° in the AWA and 4% in the AWS. In contrast to this common assumption, recent research has shown an increase in the drive force by heeling the boat a few degrees [13, 23]. The present work shows a significant drive force increase at 10° heel for the A1 and A2 which is in accordance with the previous research.

Figure 4 shows *CxSA* for the 3 sails at 3 heel angles. The A3 gives the largest drive force when upright but the drive force decreases quickly when the model is heeled over past 10°. The A1 and A2 show an increase in the *CxSA* up to a heel angle of 10°, and the A1 does not show a significant reduction in *CxSA* even at 20° heel. The A2 shows an intermediate trend: *CxSA* increases at 10° heel like the A1, and then quickly decreases when heeled past 10° like the A3. As a consequence, the A3 should be sailed upright otherwise the drive force would

drop off. The A2 can be sailed up to moderate heels, and the A1 is the best sail at 20° heel.

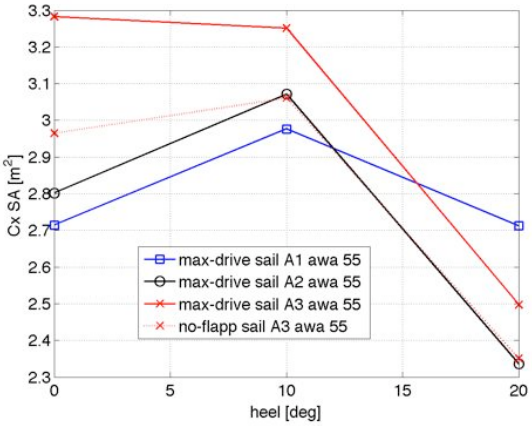

Figure 4: *CxSA* measured for sails A1, A2 and A3 at 0°, 10° and 20° heel at 55° AWA.

Figure 5 shows *CMxSA* for the 3 sails at 3 heel angles. The A3 gives the largest *CMxSA*, which decreases as the model heels to leeward. The A1 shows the lowest *CMxSA* also decreasing with increasing heel angle, and the A2 shows an intermediate trend. It can be noted that the drive-force increase at 10° heel for the A1 and A2, does not correspond to a roll-moment increase as well.

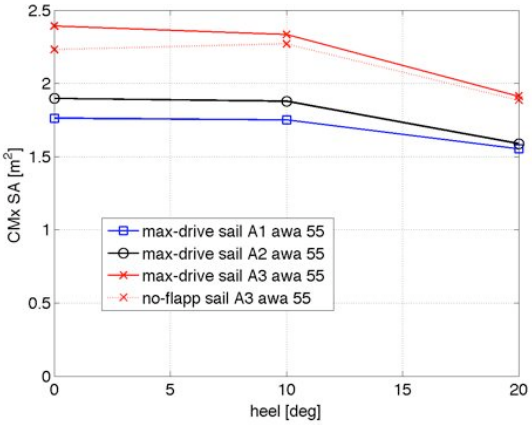

Figure 5: *CMxSA* measured for sails A1, A2 and A3 at 0, 10° and 20° heel at 55° AWA.

4.3 Sail Characterisation

The following conclusions may be drawn from the results presented in the above figures:

i. The A1 should be sailed in light air, when to maximise the VMG the closest AWA's are sailed to give a higher AWS. The higher AWS heels the boat and a sail that produces a low roll moment and does not lose drive force with heel is necessary for best performance.

ii. The A2 should be sailed in medium air, with the AWA between 40° and 55°. The moderate rolling moment would hopefully heel the boat to around 10° which would increase the drive force.

iii. The A3 should be sailed in heavy air, when to maximise the VMG the highest AWA's are sailed to minimise the distance to the leeward mark.

iv. If the wind speed increases further and the course to be sailed is closer than 70° AWA, then the large roll moment of the A3 would heel the boat excessively and consequently the driving force would drop off. In this condition, wearing the A2 would allow a reduction of *CMxSA* that would decrease the heel and take advantage of the maximum *CxSA* achieved by the A2 at moderate heel angles. Note that this situation would be unrealistic for an AC race with its windward/leeward course.

4.4 Pressure Distributions on Asymmetric Spinnakers

As discussed in the next section, the maximum drive force might be achieved when having a flapping luff induces an unstable pressure distribution. On the other hand, when the trim is changed by tightening the sheet just enough to stabilise the sail, the pressure distribution becomes stable and the following trends can be seen.

The pressure distributions on the spinnakers show differences between the 3 sails and the several sailing conditions, but general trends can be described. Figure 6 is a sketch of the pressure distributions on the 5 measured sail sections along the chord-lines. Note that the pressure coefficient axes are orientated with negative pointing upwards and the x-axis represented by the chord (light grey) is not horizontal. On the highest section the pressure has a negative peak (suction) at the leading edge followed by a slow and almost linear pressure recovery up to the trailing edge. On a conventional aerofoil with attached flow, a steep and almost linear pressure recovery is typically measured on the leeward side [24, 25]. On the contrary, a smooth or constant negative pressure coefficient is measured in fully separated conditions [26], which leads to a negative pressure coefficient at the trailing edge. The slow pressure recovery and the negative pressure coefficient measured at the trailing edge suggest that the flow is fully separated there. Moreover, the dynamic behaviour of the tell-tails observed during the test also suggests that the flow is fully separated (Figure 7).

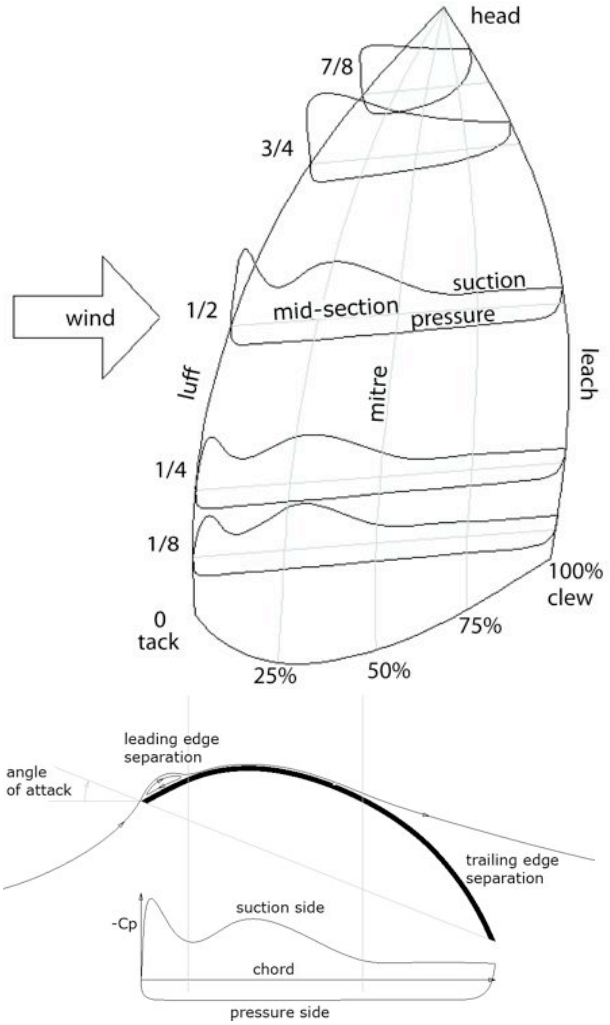

Figure 6: Schematic diagram of the pressure distribution over the asymmetric spinnakers at 5 horizontal heights and the corresponding flow field.

Figure 7: Photo of the leeward side of the A1 at 55° AWA and 10° heel.

On the middle and the lower sections the pressure distribution exhibits similar behaviour: a suction peak at the leading edge is followed by a quick pressure recovery with a local minimum suction around 10% of the curve length. The pressure recovery is correlated to the separation bubble formed behind the sharp edge of the luff [25, 26] and the re-attachment location is just in front of the local maximum pressure [26] location. Downstream of the re-attachment, the pressure decreases again due to the section curvature, showing a suction peak at a location between 10% and 40% of the curve length. After the pressure recovery, the pressure becomes constant due to the trailing edge separation [24].

As an example, Figure 8 shows the pressure coefficients, *Cp,* on the leeward side of the A1 sailing at 55° AWA and 10° heel. The flow on the top two sections is mainly separated. On the other sections, a leading edge separation with reattachment in the first 10% of the curve length is evident. Trailing edge separation occurs between 70% of the curve length (middle section), and 50% of the curve length (lowest section).

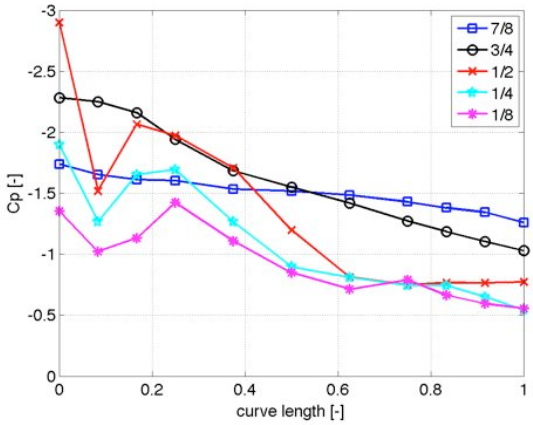

Figure 8: *Cp* measured at 7/8, 3/4, 1/2, 1/4, 1/8 of the mitre height on the leeward side of the A1.

The pressure side of the spinnaker has similar pressure distributions at various heights and conditions. The pressure coefficient at the leading edge quickly increases to a value of 1 and then remains almost constant for most of the curve length. The pressure coefficient is 1 at the stagnation point [24], because the dynamic pressure is zero and the total pressure is equal to the static pressure. For each sailing condition, the maximum pressure measured is *Cp*=1, which suggests that the chosen location for the reference pressure was adequate.

Figure 9 and Figure 10 show the effect on forces and pressures of successive sheeting-in trims of the spinnaker A1, achieved by tightening the spinnaker sheet by similar amounts from trim #1 to trim #7, at 55°AWA and 10° heel. Hence the correlation between forces, pressures and attached/separated flow is shown. The spinnaker, sailing at 55° AWA and 10° heel, is trimmed to a close-to-collapse condition, named trim #1. Then the sail sheet is tightened in successive steps from trim #2 to trim #7. Figure 9 shows that the maximum drive condition is achieved with trim #2 and successively the drive force decreases gently and does not present an abrupt drop-off. Figure 10 shows the pressure coefficients measured at the mid-section on both sides of the sail. The drive force in figure 9 and the leeward pressures in figure 10 are referred to the sail A1. Conversely, the windward pressures were measured on the sail A3. Different sails were used for technical reasons but the authors believe that the windward side pressures are very similar for every trim setting and most likely very similar across sails.

On the leeward side, trim #1 shows a pressure distribution that is affected by excessive luff flapping which increases the leading edge pressure. In fact the movement of the luff moves the pressure tap that is closest to the leading edge alternatively to the pressure and to the suction side of the sail. As a consequence, the average measured *Cp* is zero. Then a minimum *Cp* of -3 is achieved between 15% and 40% of the curve length, followed by a pressure recovery up to 80% of the curve length. The constant pressure in the last 20% of the curve length suggests a trailing edge separation. Sheeting the sail tighter with trim #2, which is the maximum drive-force trim, shows a pressure recovery in the first 5% of the curve length that suggests a leading edge separation bubble. The following suction peak is slightly smaller than that for the previous trim. Over-sheeting the sail, in trim #3, causes the leading edge suction peak to reach a *Cp* smaller than -3. The minimum *Cp* occurs under the separated boundary layer before the reattachment point at 10% of the curve length. The leading edge separation affects the following suction peak, which becomes significantly lower than for the previous trims. The trailing edge separation point moves forward to 70% of the curve length, where-after the pressure becomes constant. More over-sheeting in trim #4 reduces the leading edge suction peak. Successive trims, from #5 to #7, show fully separated flows and reduced suctions on the leeward side of the sail.

On the windward side the pressure coefficients do not vary significantly. The pressure coefficients are already close to 1 in the forward-most pressure measurement location, which is about 5mm from the leading edge. Then they remain constant for most of the curve length and decrease in the last 20% of the curve length becoming negative.

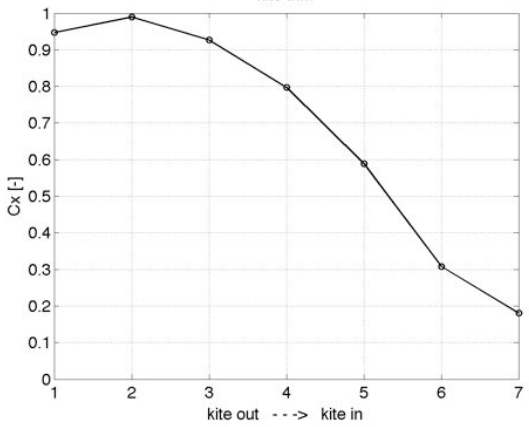

Figure 9: *Cx* corresponding to 7 consecutive trims.

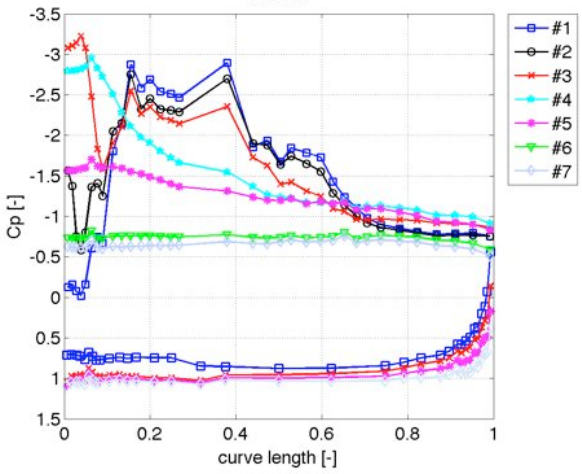

Figure 10: *Cp* vs. curve length for 7 consecutive trims.

The pressure distribution did not change significantly during the acquisition time, showing that the reattachment point after the leading edge separation and the separation point on the trailing edge do not move significantly along the curve length. In particular, the standard deviation of the pressure measurements was generally less than 1/3 of the mean pressure value. It was larger in the separated regions and lower in the attached regions but while the separation point can be detected from the mean pressure distribution, the standard deviation did not abruptly increase near the separation point.

4.5 Focus on Maximum Drive and Non-Flapping Trims

The maximum drive force is achieved when the luff flaps or is close to flapping. If the sail is over-eased, the luff stops flapping, the luff becomes stable and the drive force drops off. If the sail is over-sheeted, the drive force decreases gently. The luff flapping is induced by the vortex shedding on the leading edge of the sail [1] and generally increases both the drive force and the roll moment. Hence, if the luff is flapping, sheeting in leads to a reduction of the roll moment but, if further over-sheeted, the side force increases significantly.

In the present investigation it was found that with the A1 and the A2 the same maximum drive force could be achieved both by flapping and non-flapping luffs. For instance, in Figure 9 and Figure 10, trims #1 and #3 show a similar drive force but the luff was flapping in trim #1 and not in trim #3.

On the contrary, for the A3 both the drive force and the roll moment increase when the luff flaps. Figure 2 and Figure 3 show that the gain in *CxSA* and *CMxSA* achieved by flapping the luff of the A3 becomes larger with increasing AWA. Figure 4 and Figure 5 show that this gain decreases with an increase in heel angle. As an example the pressure measurements on the leeward side of the A3, sailed at 70° AWA and 10° heel, are shown in Figure 11. The pressure coefficient and the standard deviation divided by the mean value are measured at the mid-section. The standard deviation measured at the first tap close to the leading edge is more than 100 times larger than at the other locations. However, the measurement of the amplitude of the pressure fluctuations is certainly affected by the long pressure tubes used which were longer than 3m. These long tubes would dampen high frequency fluctuations. Conversely, moving tubes would add to the measured pressure fluctuations, although should not change the mean. In the present investigation the measured luff flapping frequency was between 1 and 2Hz.

The mean pressure trends of the flapping and non-flapping conditions of the A3 (Figure 11) are similar to the trends of the flapping and non-flapping conditions of the A1 (Figure 10, trim #1 and trim #2 respectively). The flapping condition always allows a higher suction peak but also a more positive pressure at the leading edge. Figure 11 shows that easing the spinnaker sheet and flapping the luff can also produce a delay in trailing edge separation, which increases the aerodynamic forces.

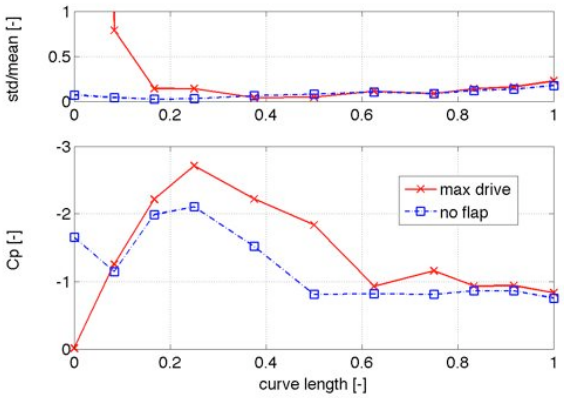

Figure 11: Standard deviation divided by the mean (above) and time-averaged pressure coefficient (below).

5. CONCLUSIONS

The aerodynamic characteristics of modern asymmetric spinnakers have been investigated and discussed. Experimental tests were performed on a 1/15th scale model in the Yacht Research Unit's Twisted Flow Wind Tunnel in preparation for Emirates Team New Zealand's challenge for the 33rd America's Cup. Three off-wind sails, named A1, A2 and A3 respectively, were tested with the same mainsail at 40°, 55° and 70° apparent wind angle at 0°, 10° and 20° heel angle. Force and moment measurements were recorded which allowed analysis of the optimum sailing condition for each sail. The following conclusions can be drawn from the analysis.

i. The A1, which has the minimum sail area and the flattest sections, gives the maximum *CxSA* and the minimum *CMxSA* at 40° AWA. Increasing the AWA causes both the drive force and roll moment to drop off, and the sail performance drops below that of the A2 and the A3. With regard to the heel angle, the drive force increases at 10° heel and slightly decreases at 20° heel. Hence the A1 can be sailed at close AWA's and in a heeled condition.

ii. The A3, which has the maximum sail area and the deepest sections, gives the minimum *CxSA* at 40° AWA but the drive force increases more than the other sails with increasing AWA. Hence it gives the maximum *CxSA* at 55° and at 70° AWA. The *CMxSA* is significantly larger than for the other two sails at every AWA and heel angle. The drive force decreases abruptly with increasing heel angle, and hence the A3 should be sailed upright at large AWA's.

iii. The A2, which has an intermediate sail area and section camber, gave values of *CxSA* and *CMxSA* part way between those of the other two sails. The

CxSA is a maximum at 10° heel and drops off at 20° heel. Hence, the A2 can perform better than the A1 and the A3 when sailing in medium conditions and with moderate heel.

A description of the pressure distribution on the asymmetric spinnakers has been given, correlating the pressure measurements with the flow field around the sails.

The pressure coefficient *Cp* on the windward side of the spinnaker is almost constant and equal to 1. *Cp* decreases to negative values near the leech.

The flow field on the leeward side of the spinnaker can be deduced from the trend in *Cp*. The following conclusions can be drawn from the pressure results.

i. A leading edge separation occurs along the entire luff of the spinnaker.

ii. The flow does not reattach on the highest sections of the sail, which leads to a negative *Cp* decreasing in magnitude slowly and almost linearly from the luff to the leech.

iii. If the luff doesn't flap, the flow reattaches on the middle and lower part of the sail, roughly in the first 10% of the curve length. This corresponds to a high suction peak near the leading edge and a pressure recovery corresponding to the reattachment point.

iv. Downstream of the reattachment point, the *Cp* shows a second suction peak due to the sail curvature.

v. If the luff flaps, the average measured *Cp* at the leading edge was 0 and the pressure peak due to the sail curvature is generally larger than when the luff doesn't flap.

vi. Trailing edge separation occurs forward of 80% of the curve length. The pressure recovery is interrupted at the separation point and the *Cp* then becomes constant at negative values.

Finally, the effect of the luff flapping was investigated. The sails designed to sail at tight AWA's (e.g. A1 and A2) do not exhibit an increase in drive force when flapping. On the contrary, the sails designed for deep angles (e.g. A3) show a significant increase in the drive force and the roll-moment when flapping. In particular, the gain achieved when flapping increases with AWA and decreases with an increase in heel angle. The trend of the *Cp* along the mid-section shows that the suction peak after reattachment increases if the luff flaps and the force increase is correlated to a delayed trailing edge separation.

6. ACKNOWLEDGMENT

The first author wants to thanks his extraordinary wife for having spent her holidays supporting him while he was testing in the wind tunnel. Her help was a fundamental contribution to this work. The support of the YRU, especially David Le Pelley and Nick Velychko is gratefully acknowledged.

7. REFERENCES

[1] MARCHAJ C. Aero-hydrodynamics of Sailing, *Dodd Mead and Company, New York,* 1979.

[2] CLAUGHTON AR & CAMPBELL IMC. Wind Tunnel Testing of Sailing Rigs. *In proceedings of the 13th International Symposium on Yacht Design and Yacht Construction (HISWA), Amsterdam, Netherlands, pp 89-106,* 14-15 November 1994.

[3] FLAY R.G.J. AND JACKSON P.S. Flow Simulation for Wind Tunnel Studies of Sail Aerodynamics, *Journal of Wind Engineering and Industrial Aerodynamics, Volume 41-44, pp. 2703-2714,* 1992.

[4] FLAY R G J. A twisted flow wind tunnel for testing yacht sails, *Journal of Wind Engineering and Industrial Aerodynamics, Volume 63, pp. 171-182,* 1996.

[5] RICHARDS PJ. The Effect of wind Profile and Twist on Downwind Sail Performance. *Journal of Wind Engineering and Industrial Aerodynamics, Volume 67&68, pp 313-321,* 1997.

[6] HANSEN H, JACKSON PS, HOCHKIRCH K. Real-Time Velocity Prediction Program for Wind Tunnel Testing of Sailing Yachts. *In proceedings of the International Conference on the Modern Yacht, RINA, Southampton, UK,* 17-18 September 2003, .

[7] ZASSO A, FOSSATI F, VIOLA IM. Twisted Flow Wind Tunnel Design for Testing Yacht Sails. *In proceedings of 4th European and African Conference on Wind Engineering (EACWE4), Prague, Czech Republic, paper#153,* 2005.

[8] FOSSATI F, MUGGIASCA S, VIOLA IM, ZASSO A. Wind Tunnel Techniques for Investigation and Optimization of Sailing Yachts Aerodynamics. *In proceeding of the 2nd High Performance Yacht Design Conference, Auckland, New Zealand, pp 105-113,* 13-16 February 2006.

[9] RANZENBACH RC, ANDERSSON P, FLYNN D. A 1997-1998 Whitbread Sail Program – Lessons Learned. *In proceedings of the 14th Chesapeake Sailing Yacht Symposium, Annapolis, MD, USA, pp 87-96,* 30 January 1999.

[10] RANZENBACH RC & MAIRS C. Wind Tunnel Testing of Downwind Sails. *In proceedings of the 14th Chesapeake Sailing Yacht Symposium, Annapolis, MD, USA, pp 171-179,* 30 January 1999.

[11] RANZENBACH RC & TEETERS J. Aerodynamic Performance of Offwind Sails Attached to Sprits. *In proceedings of the 15th Chesapeake Sailing Yacht Symposium, Annapolis, MD, USA, pp 181-192,* 26-27 January 2001.

[12] TEETERS J & RANZENBACH RC. Changes to Sail Aerodynamics in IMS Rule. *In proceedings of the 16th Chesapeake Sailing Yacht Symposium, Annapolis, MD, USA,* 21-22 March 2003.

[13] LE PELLEY D, EKBLOM K, FLAY RGJ. Wind Tunnel Testing of Downwind Sail. *In proceeding of the 1st High Performance Yacht Design Conference, Auckland, New Zealand,* 2-6 December, 2002.

[14] RICHARDS PJ, LE PELLEY D, CAZALA A, MCCARTY M, HANSEN H, MOORE W. The Use of Independent Supports to Semi-Rigid Sails in Wind Tunnel Studies. *In proceeding of the 2nd High Performance Yacht Design Conference, pp 114-122,* 13-16 February 2006.

[15] RICHARDS PJ, JOHNSON A, STANTON A. America's Cup Downwind Sails – Vertical Wings or Horizontal Parachutes?, *Journal of Wind Engineering and Industrial Aerodynamics, Volume 89, pp 1565-1577,* 2001.

[16] LASHER WC, SONNENMEIER JR, FORSMAN DR, TOMCHI J, The Aerodynamics of Symmetric Spinnakers, *Journal of Wind Engineering and Industrial Aerodynamics, Volume 93, pp 311-337,* 2005.

[17] LASHER WC & RICHARDS PJ. Validation of Reynolds-Averaged-Navier-Stokes Simulations for International America's Cup Class Spinnaker Force Coefficients in Atmospheric Boundary Layer, *Journal of Ship Research, Volume 51 (1), pp 22-38,* 2007.

[18] RICHARDS PJ & LASHER WC. Wind Tunnel and CFD Modelling of Pressures on Downwind Sails. *In proceedings of the 6th International Colloquium on Bluff Bodies Aerodynamics & Applications, Milan, Italy,* 20-24 July 2008.

[19] VIOLA IM. Downwind Sail Aerodynamics: a CFD Investigation with High Grid Resolution. *Journal of Ocean Engineering. doi:10.1016/j.oceaneng.2009.05.011,* 2009.

[20] VIOLA IM, PONZINI R, PASSONI G. Downwind Sail Aerodynamics: Large Scale Computing vs. Large Scale Wind Tunnel Test. *Journal of Wind Engineering and Industrial Aerodynamics.* Submitted April 2009.

[21] VIOLA IM. Fluidodinamica Numerica e Sperimentale Applicata alla Dinamica dell'Imbarcazione. *PhD Thesis, Politecnico di Milano, Italy,* 2 October 2008.

[22] JACKSON PS. Modelling the Aerodynamics of Upwind Sails. *Journal of Wind Engineering and Industrial Aerodynamics, Volume 63, pp 17-34,* 1996.

[23] TEETERS J. The Story So Far. *Seahorse Magazine, The Official Magazine of the Royal Ocean Racing Club, Fairmead Comunications Ltd, pp 36-39,* July 2007.

[24] THWAITES B. Incompressible Aerodynamics. Dover Publications Inc, New York. ISBN: 0-486-65465-6, 1969.

[25] ABBOT IH & VON DOENHOFF AE. Theory of Wing Section. *Dover Publications Inc, New York. ISBN: 0-486-60586-8,* 1949.

[26] CROMPTON MJ & BARRET RV. Investigation of the separation bubble formed behind the sharp leading edge of a flat plate at incidence. *Proceedings of the Institution of Mechanical Engineers, Part G: Journal of Aerospace Engineering (ISSN 0954-4100), Volume 214, (3), pp 157-176,* 2000.

Grant Spanhake

Thanks for letting me review your paper.
Great job, I found it very informative and helpful.

I do have some comments and questions on the paper.

Page 3, Table 1: I would suggest adding a Mid girth # or mid girth % to the table (See page 5 comments).
3.3: It would be good to see a close up photo of the pressure taps.
3.3: At a later date it would be good to see the results of (Twisted vanes verses non-twisted).

Page 5, Figure 4: I found it interesting that the A-3 Cx SA forces does not increase at 10 degrees of heel like the other sails. I can only think the reason for this is that the wider mid-girth (reason for adding it to Table 1) may interfere with the mainsail/Slot/up-ward flow?

Page 7: One good addition would be add the timing of the flaps eg below. This will give a sail trimmer some practical guidelines and consistency.

Kite out(1) –in (7)	# of flaps per 10 sec's	Cx	m/s	Comments
1	10	0.95	3.5	Sail very un-stable
2	5	1.0	3.5	Sail just flicking
3	1 (Curling)	1.05	3.5	Sail curling
4	0	0.9	3.5	Sail stable
5	0	0.8	3.5	Start to be over-trimmed
6	0	0.6	3.5	Over-trimmed
7	0	0.3	3.5	Over-trimmed

Page 8, 4.5: "*In the present investigation it was found that with the A1 and the A2 the same maximum drive force could be achieved both by flapping and non-flapping luffs. For instance, in Figure 9 and Figure 10, trims #1 and #3 show a similar drive force but the luff was flapping in trim #1 and not in trim #3.*"

I suspect that this could be explained with the red items above. I had originally thought that the reason for this may have been, that the wind speed was set too high. But at 3.5 m/s (6.80 TWS) I don't think this is the case.

Conclusion: I would believe your findings and conclusions based on real world on the water and wind tunnel experience.
It would be interesting to further investigate the following.

a) Twisted vanes verses non-twisted.
b) Flicking luff verses curling luff

c) Keep the same sail area and increase/reduce the mitre depth at 400 to see if there is a sweet spot.

Thank you

William Lasher

The authors present a very nice investigation of asymmetric spinnakers by providing detailed surface pressure measurements and analyzing them from both a flow and overall force perspective. Their discussion regarding the effect of luff flapping on the pressures and forces was particularly interesting, as this has an important impact on sail trim. I am curious as to why the flatter spinnakers produced a higher drive force when over trimmed (trim #2), whereas the fuller spinnaker did not. Is it due to a higher peak suction pressure for sail A3, or a larger delay in trailing edge separation compared to sail A1? Perhaps an overlay of the Cp difference from sail A1 onto Figure 11 would help to answer this question.

Also, was there anything in the pressure measurements that explains the results shown in Figure 4? Specifically, why does the drive force increase for sails A1 and A2 at 10 degrees heel, and decrease for sail A3? I recognize that this may be difficult to determine from pressure measurements alone, but any comments from the authors would be appreciated.

Robert Ranzenbach

The authors are to be congratulated on their meticulous effort to obtain pressure measurement data on a flexible membrane like an asymmetric spinnaker. As noted in the paper, much of the experimental evidence collected to date has been focused on global aerodynamic forces and this additional data will prove invaluable to our understanding of the underlying physics of asymmetric spinnakers and to anyone interested in validating their CFD predictions of this complex, three-dimensional, separated flow.

Not only does it appear that great care was taken to collect data, it is clear that the authors took great pains to present the results in a compact but meaningful fashion as evidenced by Figure 6 which is an especially good qualitative representation of the pressure results and provides an excellent template for any subsequent CFD validation efforts that might follow.

I do feel compelled to comment on one additional element of the paper. I understand that Figures 9 and 10 are an amalgam of results, Cx and leeward side pressure from sail A1 but windward side pressure from sail A3. The presentation may have been better served if the leeward side A1 and windward side A3 pressure results had been shown on different graphs rather than relying upon the undocumented assertion that the windward side pressures are very similar for every trim setting. In addition, greater comment might be offered by the Authors on the important differences that are evidenced on the windward side between trim condition #1 which shows the windward side Cp varying greatly from the nearly constant value of 1 that dominates the results for nearly every other trim condition. It also seems that these results are not consistent with a claim made earlier in the paper regarding the Cp maximum being equal to or less than 1.0 everywhere.

I am sure that like me, others in the sail testing/design community will look forward to the next installment promised by the authors to discuss how twisted flow changes the pressure distribution on the spinnaker. I personally hope that they will not limit their data collection

and analysis to only one uniform and one twist profile so that the impact of varying twist profiles may also be illuminated.

Michael Richelsen

I would like to applaud the authors for their work and bringing it into the public.

The measured pressure sections help understand the amount of attached flow on the sails. This is valuable not just for feeding back information from a test to the sail designer, as it also allows for more detailed comparison with CFD results. Without the pressure measurements CFD results can only be compared on the basis of total forces whereas now, given measured section pressure values, one can get a better understanding of how well the simulated flow field in the CFD matches the tunnel flow. This is a valuable aid in improving CFD based predictions, which is becoming another tool for evaluating the performance of a sail design.

Obviously to do such a tunnel versus CFD comparison one will also need to obtain an accurate 3D geometry of the flying shape corresponding to a set of pressure measurements. Presumably the tunnel at the Auckland University already has capabilities in this field, either by laser scanning or photogrammetry ?

Ignazio Maria Viola & Richard Flay

Thank you for the generous comments and the very interesting points highlighted. The sail aerodynamics is still far from being fully understood and we hope that this paper answered some questions, but we are conscious that it also raised many other questions.

The large amount of data collected in the presented experiments couldn't be fully discussed due to the restricted space available. Hence, a new manuscript titled Pressure Distributions on Modern Asymmetric Spinnakers has been submitted to the Journal of Small Craft Technology, where the pressure distribution on five sections of the three sails is discussed.

In particular, the effect of the twisted flow is discussed. The pressure measured on three horizontal sections of the sail A3 sailing at 55° AWA and 10° heel, both with and without the twisted flow, is presented. With regard to the question raised by Robert Ranzenbach, only one twisted flow profile was tested due to the time demand of the test.

The effect of the heel on the pressure distribution over the five sail sections is discussed, which shows the strong three-dimensionality of the phenomena. For instance, heeling the A2 by 10° causes the pressure to increase on the highest sections, and to decrease on the lowest sections. Some hypothesis and some possible interpretations are highlighted. With regard to the comment by Grant Spanhake, the different behaviour of the three sails can be due to the mid-girth interference with the mainsail. The mid girths of the A1, A2 and A3 are 1.21m, 1.35m, and 1.61m respectively. Hence, the A3 has the maximum absolute mid girth and also the maximum mid-girth/foot ratio. However, the deeper mitre and the longer sections can significantly affect the complex three-dimensional phenomena, which can explain the opposite trend of the A3 compared to the A1 and A2. Moreover, heeling the model, the spinnaker sheet can be eased without causing the sail to collapse. The sheet ease changes the sail geometry, which is correlated with the force increase. Hence, the way the geometry changes can also explain the trend differences.

Some clarifications are necessary about the flapping and non-flapping trims. With regard to the comment by William Lasher, the non-flapping luff leads to a significant force reduction in the A3 because it is correlated to a significant increase in separated flow. In fact, figure 11 of the paper shows the separation point of the A3 moving from roughly the 60% of the chord to roughly the 50% of the chord, when the sheet is tightened to stabilize the luff. The anticipated trailing edge separation leads to a significant reduction of the suction after the turbulent reattachment. Conversely, the flapping and non-flapping trims of the A1, named trim #1 and #3 respectively in figure 10 of the paper, show similar pressure suction and trailing edge separation. In particular, with regard to the comment by Grant Spanhake, the luff flaps at 1.4 Hz in trim #1, while does not flap in all the other trims. Figure 1 shows the auto-correlation of the pressure signal measured on the leeward side at the leading edge for the three trims #1, #2 and #3.

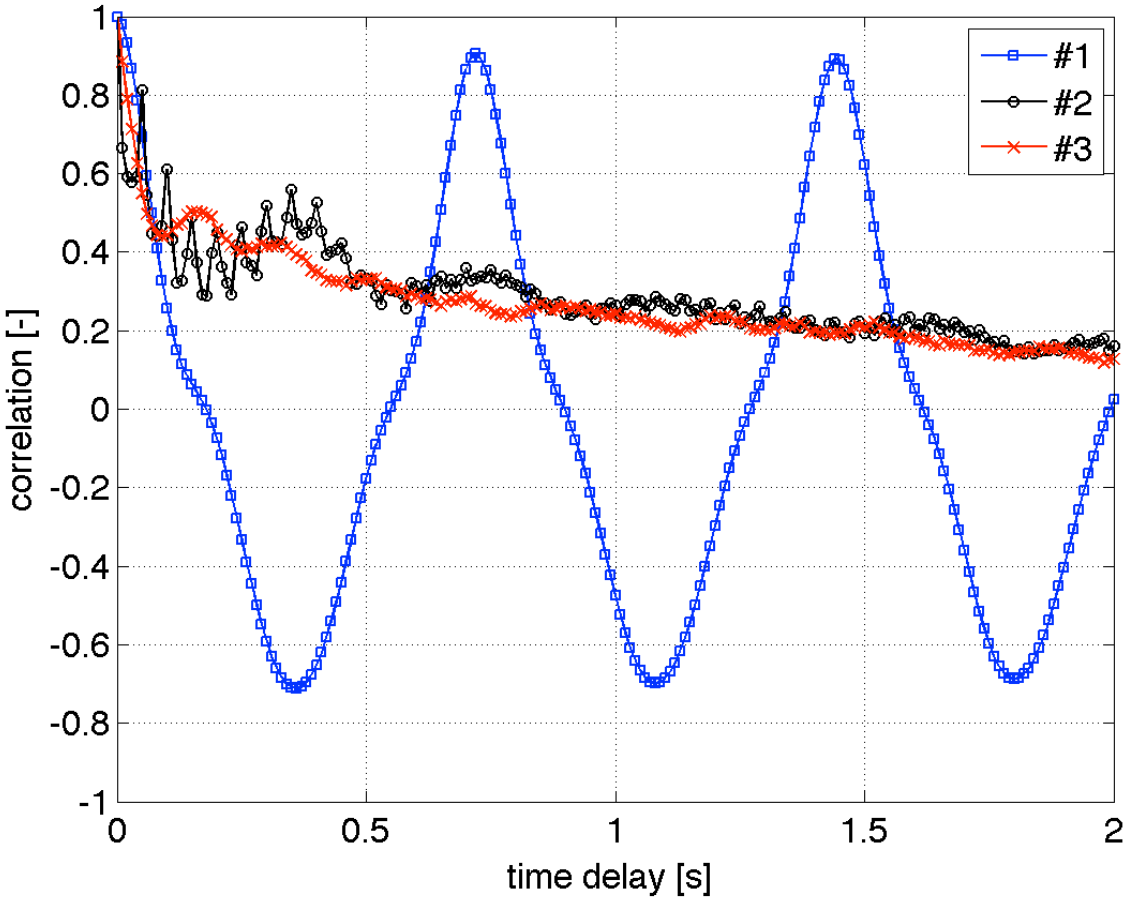

Figure 1: Auto-correlation of the pressure signals for three trims.

The drive force achieved by trim #1 is lower than the drive force achieved by trim #2. However, in the unstable full-scale condition, trim #2 and trim #3 might be unrealistic, because to stabilize the luff, the sheet has to be tightened significantly (as in trim #4). Hence, in full-scale condition the flapping trim would result in a larger drive force than the non-flapping trim.

With regard to the comment by Robert Ranzenbach, the pressure coefficient measured on the windward side of the A3 is presented on figure 10 of the paper for four trims, named #1, #3, #5 and #7 respectively. The luff is flapping in trim #1, while the sheet is tightened enough to stabilize the luff in trim #3, and it is over-trimmed in trim #5 and #7. When the luff is not flapping, the pressure coefficient is almost one over the whole section, id est at

the same pressure of the stagnation point. When the luff flaps, the stagnation point moves from the windward to the leeward side and vice versa repeatedly. When the stagnation point is on the leeward side, the pressure coefficient over the windward side should be lower than one, due to the higher velocity of the flow. Hence, a flapping trim leads to two values of the pressure coefficient: one when the luff is straight the pressure coefficient is almost 1.0, and another when the luff is curled the pressure coefficient is lower than 1.0. The pressure coefficient during flapping trim results in the average of these two values, which would be lower than 1.0. In fact, the pressure coefficient correlated to trim #1 is roughly Cp=0.7.

With regard to the comments by Michael Richelsen, the test was performed also with the aim to provide suitable CFD benchmarks, and cameras recorded each trim from many points of view to allow the flying shapes to be post-processed with photogrammetric technique. The Yacht Research Unit is consistently investing in flying shape detecting systems, and is developing a real-time photogrammetric system named VSPARS, which is already used for commercial testing, and increasing the capabilities of an existing devoted laser scanner.

With regard to the comments by Grant Spanhake, figure 2 shows one of the pressure tap adopted. The tap is a truncated cone with a rectangular base, the base of which is 17x10 mm^2. The transparency of the material allows the hole on the base to be seen, and is connected with a stainless steel tube to a plastic pressure tube.

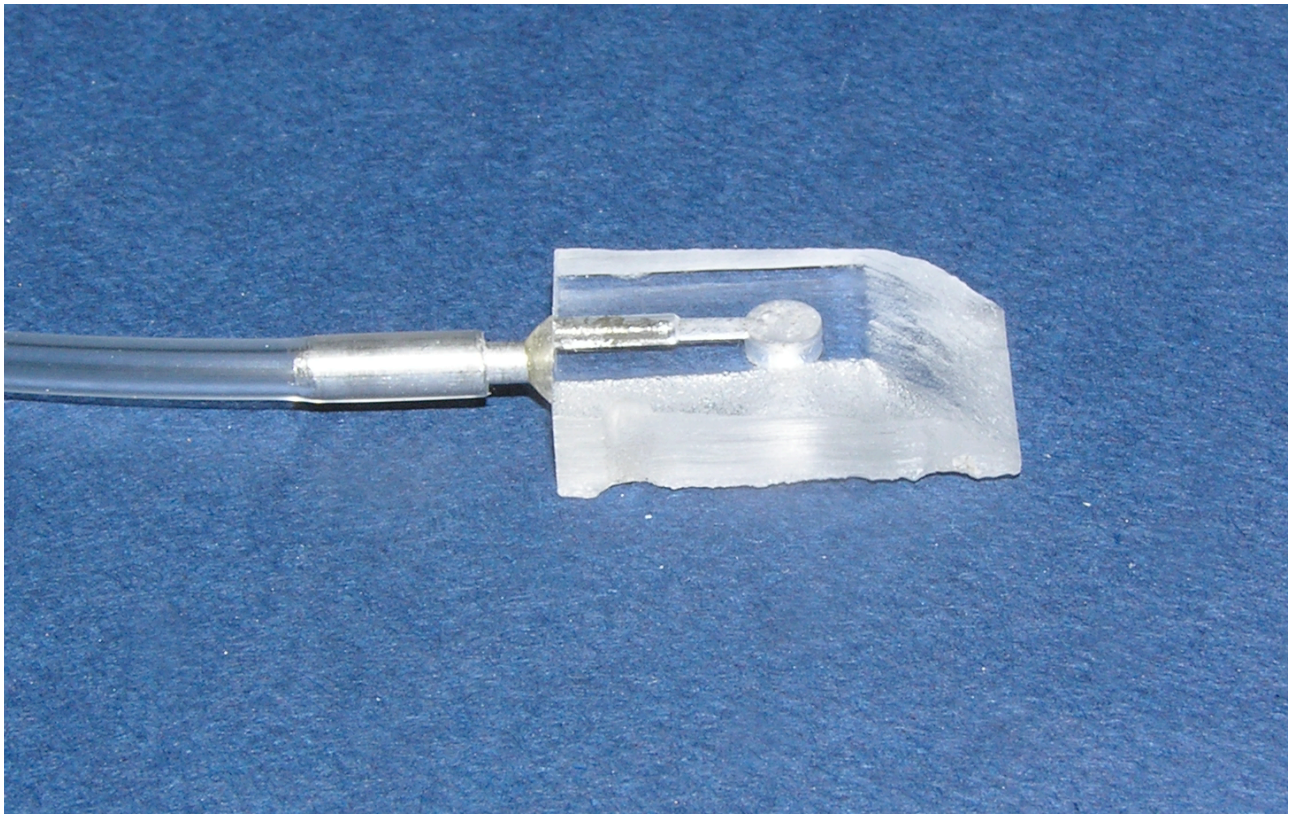

Figure 1: Photograph of the pressure tap.

We thank the reviewers for their insightful and interesting comments about our paper. We will take note of their input in our future research on this topic.